

Single crystals of DPPH grown from diethyl ether and carbon disulfide solutions — Crystal structures, IR, EPR and magnetization studies

Dijana Žilić^{a,*}, Damir Pajić^b, Marijana Jurić^a, Krešimir Molčanov^a, Boris Rakvin^a, Pavica Planinić^a, Krešo Zadro^b

^a*Ruđer Bošković Institute,
Bijenička cesta 54, 10000 Zagreb, Croatia*
^b*Department of Physics, Faculty of Science, University of Zagreb,
Bijenička cesta 32, 10000 Zagreb, Croatia*

Abstract

Single crystals of the free radical 2,2-diphenyl-1-picrylhydrazyl (DPPH) obtained from diethyl ether (ether) and carbon disulfide (CS₂) were characterized by the X-ray diffraction, IR, EPR and SQUID magnetization techniques. The X-ray structural analysis and IR spectra showed that the DPPH form crystallized from ether (DPPH1) is solvent free, whereas that one obtained from CS₂ (DPPH2) is a solvate of the composition 4 DPPH · CS₂. Principal values of the *g*-tensor were estimated by the X-band EPR spectrometer at room and low (10 K) temperatures. Magnetization studies revealed the presence of antiferromagnetically coupled dimers in both types of crystals. However, the way of dimerization as well as the strength of exchange couplings are different in the two DPPH samples, which is in accord with their crystal structures. The obtained results improved parameters accuracy and enabled better understanding of properties of DPPH as a standard sample in the EPR spectrometry.

Keywords: DPPH, crystal structure, diethyl ether, carbon disulfide, EPR, magnetization

1. Introduction

The stable aromatic free radical 2,2-diphenyl-1-picrylhydrazyl (DPPH) is one of the first and most widely used standard samples for determination of the *g*-factors of the spin species and for measuring the unpaired spin concentration using electron paramagnetic resonance (EPR) [1]. DPPH was synthesized in 1922, and its EPR spectrum was recorded for the first time in 1950 [2]. Chemical stability of DPPH and its very narrow spectral line have led to the widespread use of the powder form of this radical as an EPR standard [3]. Single crystals of DPPH are also frequently used in EPR spectroscopy because the linewidth they produce is considerably narrower than that of the powder form.

Various types of DPPH crystals have been prepared up to now — some of them are solvent free and some contain molecules of solvation [4]. In the Cambridge Structural Database [5] crystal structures of two DPPH solvates, one with acetone [6] and the other with benzene [7], are deposited. The benzene solvate was also

investigated by neutron diffraction [3]. Some preliminary X-ray diffraction measurements, done by Williams [8], indicated that the DPPH crystal forms obtained from diethyl ether (ether; orthorhombic crystal system) and carbon disulfide (CS₂; triclinic crystal system) were both solvent free. However, their crystal structures have never been solved, i.e. no atomic coordinates have been deposited in the Cambridge Structural Database [5].

More recently, a new application of DPPH — in detecting local fields in the close vicinity of the surface of superconductors [9, 10] and single molecule magnets [11] — has been established in our laboratory. These results prompted us to investigate the properties of DPPH in more details.

In this paper, we report on the single-crystal X-ray diffraction study, as well as the IR, EPR and SQUID magnetization measurements of the two Williams' "solvent-free" forms [8] of DPPH, i.e. the one grown from ether (DPPH1) and the other form crystallized from CS₂ (DPPH2). A detailed structural analysis showed that the orthorhombic DPPH form (crystallized from ether), in accord with the previous preliminary measurements [8], does not really contain solvent molecules; however, the triclinic DPPH form (crys-

*Corresponding author. Fax: + 385 1 4680 245.
Email address: dzilic@irb.hr (Dijana Žilić)

45 tallized from CS₂), believed to be solvent free for
46 40 years, is actually a solvate with the stoichiometry
47 4 DPPH · CS₂. This form is isostructural with the ace-
48 tone solvate, 4 DPPH · CH₃COCH₃ [6]. In addition, it
49 has been shown that magnetic properties of these two
50 kinds of DPPH crystals are quite different.

51 2. Material and methods

52 2.1. Materials

53 DPPH was purchased from commercial sources and
54 used without further purification. Elemental analysis for
55 C, H and N was carried out using a Perkin Elmer Model
56 2400 microanalytical analyzer.

57 2.2. Preparation of the single crystals

58 **DPPH1.** Crystals of DPPH1 were grown from a so-
59 lution of DPPH in ether. The tightly closed reaction
60 beaker was kept in a refrigerator. The dark needle-like
61 crystals were obtained after two days. Anal. calcd for
62 C₁₈H₁₂N₅O₆ (*M_r* = 394.33): C, 54.83; H, 3.07; N,
63 17.76. Found: C, 54.48; H, 3.32; N, 17.62%. IR data
64 (KBr): $\tilde{\nu}$ = 3085 (w), 3071 (vw), 1598 (s), 1575 (s),
65 1523 (s), 1479 (m), 1460 (w), 1453 (w), 1434 (w), 1408
66 (w), 1324 (vs), 1292 (sh), 1212 (s), 1171 (m), 1073 (s),
67 1024 (w), 997 (w), 952 (m), 935 (w), 914 (m), 908 (sh),
68 842 (w), 833 (sh), 819 (w), 787 (m), 755 (s), 740 (m),
69 724 (m), 712 (m), 703 (m), 698 (m), 686 (s), 653 (w),
70 620 (w), 578 (w), 557 (w), 523 (w), 509 (w), 462 (w),
71 440 (w), 420 (w), 371 (w), 308 (w) cm⁻¹.

72 **DPPH2.** Crystals of DPPH2 were grown from a solu-
73 tion of DPPH in CS₂. The tightly closed reaction beaker
74 was kept in a refrigerator. The dark needle-like crys-
75 tals were formed in a period of six days. Anal. calcd
76 for C₁₈H₁₂N₅O₆·0.25CS₂ (*M_r* = 413.36): C, 53.03; H,
77 2.93; N, 16.94. Found: C, 52.78; H, 3.12; N, 16.79%.
78 IR data (KBr): $\tilde{\nu}$ = 3087 (w), 3069 (vw), 1597 (s), 1574
79 (s), 1539 (m), 1525 (m), 1512 (s), 1478 (m), 1462 (w),
80 1453 (w), 1439 (w), 1412 (w), 1326 (vs), 1292 (m),
81 1210 (m), 1171 (m), 1073 (s), 1025 (w), 996 (w), 951
82 (m), 936 (w), 914 (sh), 909 (m), 844 (sh), 832 (w), 819
83 (w), 787 (w), 765 (sh), 757 (s), 739 (m), 715 (s), 703
84 (s), 698 (sh), 688 (m), 680 (m), 646 (w), 616 (w), 581
85 (w), 560 (w), 507 (w), 460 (w), 434 (w), 425 (w), 359
86 (w), 305 (w) cm⁻¹.

87 2.3. Physical techniques

88 **Crystallography.** Single crystals of DPPH1 and
89 DPPH2 were measured on an Oxford Diffraction Xcal-
90 ibur Nova diffractometer with a microfocus copper tube
91 (CuK_α radiation) at room temperature (*T* = 293 (2) K).

92 Lowering the temperature drastically increased mosaic-
93 ity, significantly degrading data quality.

94 CrysAlis PRO [12] program package was used for
95 data reduction. The structures were solved with
96 SHELXS97 and refined with SHELXL97 [13]. The
97 models were refined using the full-matrix least-squares
98 refinement. All atoms except hydrogen were refined
99 anisotropically; hydrogen atoms were located from
100 the difference Fourier map and refined as riding en-
101 tities. The atomic scattering factors were those in-
102 cluded in SHELXL97 [13]. Molecular geometry calcu-
103 lations were performed with PLATON [14], and molec-
104 ular graphics were prepared using ORTEP-3 [15] and
105 CCDC-Mercury [16]. Crystallographic and refinement
106 data for the structures reported are shown in Table 1.

107 Supplementary crystallographic data for this paper
108 can be obtained free of charge via
109 www.ccdc.cam.ac.uk/conts/retrieving.html (or from the
110 Cambridge Crystallographic Data Centre, 12, Union
111 Road, Cambridge CB2 1EZ, UK; fax: +44 1223
112 336033; or deposit@ccdc.cam.ac.uk). CCDC 732147
113 & 732148 contain the supplementary crystallographic
114 data for this paper.

115 **IR spectroscopy.** Infrared spectra were recorded as
116 KBr pellets on an ABB Bomem FT model MB 102
117 spectrometer, in the 4000–200 cm⁻¹ region.

118 **EPR spectroscopy.** EPR measurements were per-
119 formed on the single crystals of DPPH1 and DPPH2.
120 Dimensions of the prepared single crystals were ap-
121 proximately 2.0 × 0.2 × 0.2 mm³. The crystals were
122 mounted on a quartz holder in the cavity of an X-
123 band EPR spectrometer (Bruker Eleksys 580 FT/CW)
124 equipped with a standard Oxford Instruments model
125 DTC2 temperature controller. The measurements were
126 performed at the microwave frequency around 9.7 GHz
127 with the magnetic field modulation amplitude of 5 μT at
128 100 kHz. The crystals were rotated round three mutu-
129 ally orthogonal axes: a crystallographic *a* axis (the crys-
130 tals of both DPPH1 and DPPH2 were elongated along
131 the *a* axes), an arbitrary chosen *b** axis perpendicular
132 to *a* and a third *c** axis, perpendicular to both *a* and *b**
133 (because of the thin needle-like form, it was difficult to
134 orientate crystals in the crystallographic *b* and *c* axes).
135 The EPR spectra were recorded at 5° steps. The rota-
136 tion was controlled by a goniometer with the accuracy
137 of 1–2°. A larger uncertainty (2–3°) was related to the
138 optimal deposition of the crystals on the quartz holder.
139 The EPR spectra were measured at two temperatures:
140 room (*T* = 297 K) and low (*T* = 10 K).

141 **Magnetization study.** Magnetization of the DPPH1
142 and DPPH2 samples in the powdered form (about
143 25 mg) was measured using a commercial MPMS5

Table 1: Crystallographic, data collection and structure refinement data.

	DPPH1	DPPH2
Chemical formula	C ₁₈ H ₁₂ N ₅ O ₆	C ₁₈ H ₁₂ N ₅ O ₆ ·0.25CS ₂
M_r / g mol ⁻¹	394.33	413.36
Color	black	black
Crystal size / mm	0.25 x 0.10 x 0.07	0.28 x 0.13 x 0.08
Crystal system	orthorhombic	triclinic
Space group	$Pn2_1a$	$P\bar{1}$
a / Å	16.7608 (7)	7.5577 (5)
b / Å	26.8351 (9)	13.5724 (7)
c / Å	7.8458 (3)	18.922 (1)
α / °	90	95.084 (4)
β / °	90	92.141 (5)
γ / °	90	101.488 (5)
V / Å ³	3528.9 (2)	1891.6 (2)
Z	8	4
D_{calc} / g cm ⁻³	1.484	1.451
Radiation	CuK α	CuK α
Data collection method	CCD	CCD
T / K	293 (2)	293 (2)
Absorption correction	none	none
Measured reflections	11143	19986
Independent reflections	3664	7590
Observed reflections ($I > 2\sigma(I)$)	2787	3908
R_{int}	0.0387	0.0545
Θ_{max} / °	76.29	76.15
Refinement	F^2	F^2
$R[F^2 > 2\sigma F^2]$	0.0674	0.0639
$wR(F^2)$	0.1746	0.2151
S	1.069	0.963
No. of reflections	3664	7590
No. of parameters	523	538
H-atom treatment	constrained	constrained
$\Delta\rho_{max}, \Delta\rho_{min}$	0.308; -0.210	0.438; -0.391

144 SQUID magnetometer. The magnetization was checked
145 to be linear with respect to the applied magnetic field up
146 to 5 T for both compounds at several temperatures (2, 5
147 and 50 K). The temperature dependence of magnetiza-
148 tion was measured in the applied magnetic fields of 0.1
149 and 1 T, in the temperature range 1.9–290 K. For each
150 particular compound, measurements in the two different
151 magnetic fields resulted with identical susceptibility vs
152 temperature curves.

153 3. Results and discussion

154 3.1. Crystallography

155 The geometries and conformations of the DPPH radicals,
156 DPPH1 and DPPH2 (Figures 1 and 2), agree well
157 with those found in previous crystallographic studies of
158 DPPH solvates [3, 6, 7]. Bond lengths and angles of
159 the pycryl–N–N–Ph₂ system (Table 2) indicate that the
160 unpaired electron is delocalized over the C1–N19–N20
161 fragment with the bonds order of *ca* 1.5. The bond or-
162 der of N20–C7 and N20–C13 is *ca* 1. Such an electronic
163 structure is in agreement with a recent DFT study [17].
164 The DPPH molecule is not rigid; however, ENDOR
165 spectroscopy [18] and DFT calculations [17] indicate
166 that restricted rotations of phenyl rings are possible in
167 solution. Therefore, the crystallographically observed
168 conformation is thermodynamically, probably, the most
169 stable one.

170 In the both DPPH1 and DPPH2 crystal structures, the
171 asymmetric unit contains two symmetry-independent
172 DPPH radicals; the asymmetric unit of DPPH2 contains
173 also a half of a CS₂ molecule (its sulphur atom is lo-
174 cated in a crystallographic inversion center). All four
175 symmetry-inequivalent molecules described in the pa-
176 per adopt the same conformation (Figure 3), already ob-
177 served in the crystal structures of several DPPH crystal
178 forms [3, 6, 7]. Crystal packings of the both structures
179 (DPPH1 and DPPH2) are dominated by the C–H...O
180 hydrogen bonds (Table 3). In DPPH2, $\pi\cdots\pi$ interactions
181 are also present (Table 4). DPPH1 forms a 3D hydrogen
182 bonded network (Figure 4), while DPPH2 forms 2D hy-
183 drogen bonded sheets parallel with (100), held together
184 by the $\pi\cdots\pi$ interactions. Such a structure is porous, with
185 channels filled with CS₂ molecules running in the direc-
186 tion [100] (Figure 5).

187 3.2. IR spectroscopy

188 The IR spectra of DPPH1 and DPPH2 show char-
189 acteristic absorption bands that can, in general, be at-
190 tributed to the presence of aromatic hydrocarbon ligands

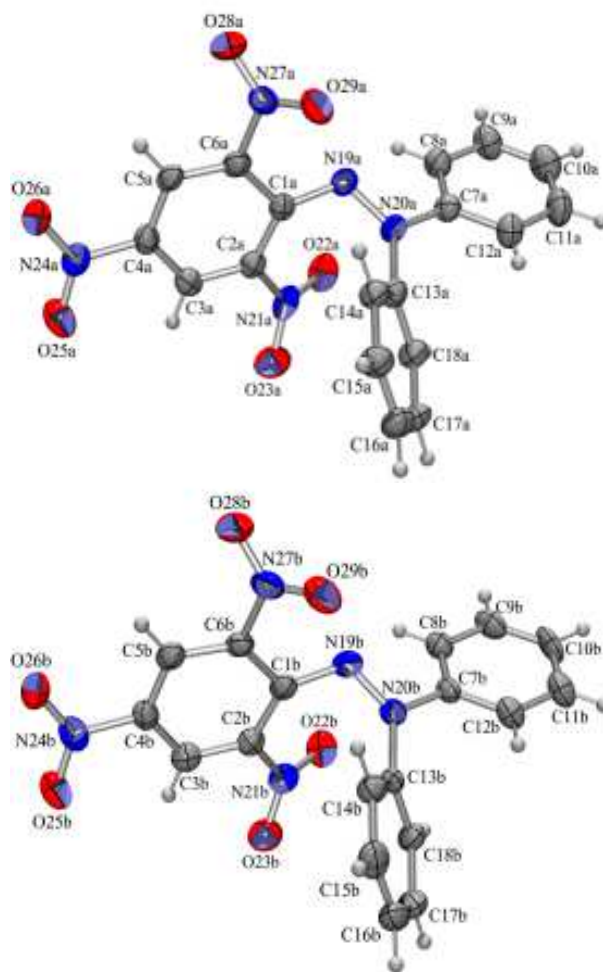


Figure 1: ORTEP-3 [15] drawing of two symmetry-independent molecules in DPPH1. Atomic displacement ellipsoids are drawn at 50% probability and hydrogen atoms are depicted as spheres of arbitrary radii. Atom numbering is the same as in other crystallographic studies [7, 6, 3]; labels **a** and **b** denote symmetry-independent molecules **a** and **b**.

Table 3: Geometric parameters of the hydrogen bonds (\AA , $^\circ$).

	$d(D-H)/\text{\AA}$	$d(H \cdots A)/\text{\AA}$	$d(D \cdots A)/\text{\AA}$	$(D-H \cdots A)/^\circ$	Symm. op.
DPPH1					
C14A–H14A \cdots O25A	0.93	2.53	3.151 (8)	125	$x, y, -1 + z$
C14B–H14B \cdots O25B	0.93	2.54	3.185 (8)	127	$x, y, -1 + z$
C17B–H17B \cdots O22A	0.93	2.53	3.400 (10)	156	$1 - x, 1/2 + y, 1 - z$
C12B–H12B \cdots O23B	0.93	2.64	3.344 (9)	145	$x, y, 1 - +z$
C8A–H8A \cdots O26B	0.93	2.61	3.278 (4)	130	$x, y, -1 + z$
DPPH2					
C14A–H14A \cdots O25A	0.93	2.61	3.355 (6)	135	$-1 + x, y, z$
C12A–H12A \cdots O23A	0.93	2.63	3.301 (5)	129	$-1 + x, y, z$
C5B–H5B \cdots O28B	0.93	2.72	3.355 (6)	127	$1 - x, 2 - y, 1 - z$
C15A–H15A \cdots O26B	0.93	2.69	3.493 (6)	145	$-1 + x, -1 + y, z$
C8A–H8A \cdots O28A	0.93	2.54	3.200 (7)	129	$-x, -y, -z$

Table 4: Geometric parameters of $\pi \cdots \pi$ interactions in DPPH2 (\AA , $^\circ$).

	$Cg^1 \cdots Cg$	α^2	β^3	δ^4	offset/ \AA	symm.op.
C1B \longrightarrow C6B \cdots C1B \longrightarrow C6B	4.027 (2)	0.00	32.17	3.409	2.144	$2 - x, 2 - y, 1 - z$
C7B \longrightarrow C12B \cdots C7B \longrightarrow C12B	3.973 (1)	0.00	20.16	3.730	1.369	$1 - x, 1 - y, 1 - z$

¹Ring centroid; ²Angle between two ring planes; ³Angle between a centroid-centroid line and a normal to the plane of the first ring; ⁴Distance between the centroid of the first ring and the plane of the second one.

Table 2: Geometric parameters of the pycryl–N–N–Ph₂ system (\AA , $^\circ$).

DPPH1		
	molecule a	molecule b
C1–N19	1.364 (8)	1.376 (8)
N19–N20	1.352 (7)	1.321 (7)
N20–C7	1.405 (8)	1.426 (8)
N20–C13	1.432 (8)	1.435 (7)
C1–N19–N20	118.0 (5)	117.0 (5)
N19–N20–C7	116.9 (5)	115.6 (5)
N19–N20–C13	121.4 (5)	123.5 (5)
C7–N20–C13	121.0 (5)	120.2 (5)
DPPH2		
	molecule a	molecule b
C1–N19	1.354 (5)	1.366 (4)
N19–N20	1.342 (4)	1.339 (4)
N20–C7	1.404 (5)	1.416 (4)
N20–C13	1.434 (5)	1.432 (4)
C1–N19–N20	118.6(3)	118.8 (3)
N19–N20–C7	115.6(3)	115.6 (3)
N19–N20–C13	122.0(3)	121.5 (2)
C7–N20–C13	121.7(3)	122.5 (2)

and nitro groups. The absorption bands of weak intensity that occur in the region 3100–3000 cm^{-1} for both compounds originate from the aromatic C–H stretching vibrations. The absorption bands of rather strong intensity at 1598, 1575 and 1479 cm^{-1} in the spectrum of DPPH1, and at 1597, 1574 and 1478 cm^{-1} in the spectrum of DPPH2 correspond to the stretch of the C–C bonds from the aromatic rings [19]. The absorption bands corresponding to the nitro groups in DPPH1 are located at 1523 cm^{-1} [$\nu_{as}(\text{NO})$], 1324 cm^{-1} [$\nu_s(\text{NO})$], 914 cm^{-1} [$\nu(\text{C–NO}_2)$] and also at 842 and 833 cm^{-1} [$\delta(\text{ONO})$]. The corresponding bands for DPPH2 are placed at 1525 cm^{-1} [$\nu_{as}(\text{NO})$], 1326 cm^{-1} [$\nu_s(\text{NO})$], 914 cm^{-1} [$\nu(\text{C–NO}_2)$] and at 844 and 832 cm^{-1} [$\delta(\text{ONO})$] [19, 20]. The presence of the solvate molecule of CS_2 in DPPH2 is confirmed by the strong absorption band at 1512 cm^{-1} [$\nu_{as}(\text{CS}_2)$] [20].

3.3. EPR spectroscopy

3.3.1. DPPH1

The EPR spectrum of DPPH1 was a Lorentzian singlet line at room temperature. The angular rotation of the single crystal gave an approximately isotropic line with the (peak-to-peak) width $W = (0.16 \pm 0.02)$ mT and $g = 2.0036 \pm 0.0001$.

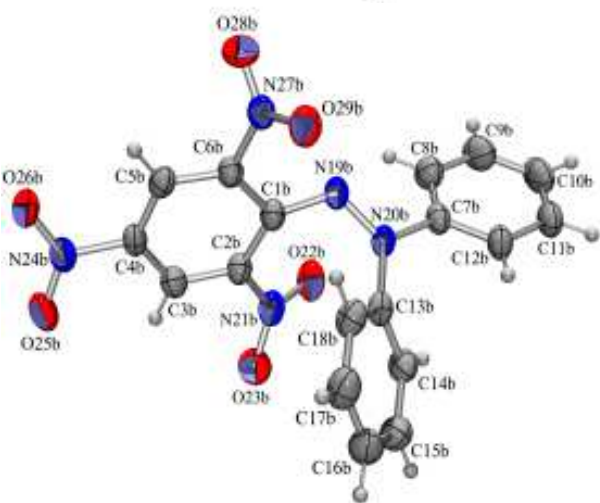
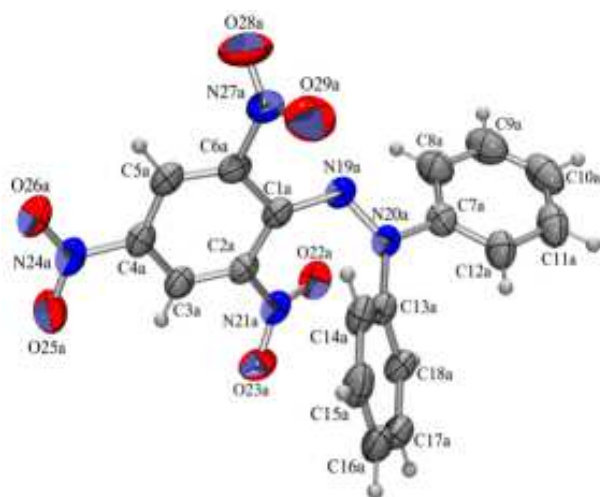


Figure 2: ORTEP-3 [15] drawing of two symmetry-independent molecules in DPPH2. Atomic displacement ellipsoids are drawn at 50% probability and hydrogen atoms are depicted as spheres of arbitrary radii. Atom numbering is the same as in other crystallographic studies [3, 6, 7]; labels **a** and **b** denote symmetry-independent molecules **a** and **b**.

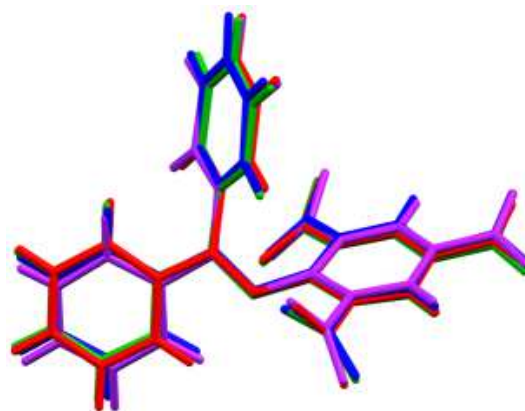


Figure 3: Overlap of four symmetry-independent molecules in the crystal structures of DPPH1 and DPPH2. The differences in conformations are almost all within 3 e.s.d.'s. Molecules **a** and **b** of DPPH1 are green and blue, while molecules **a** and **b** of DPPH2 are red and purple.

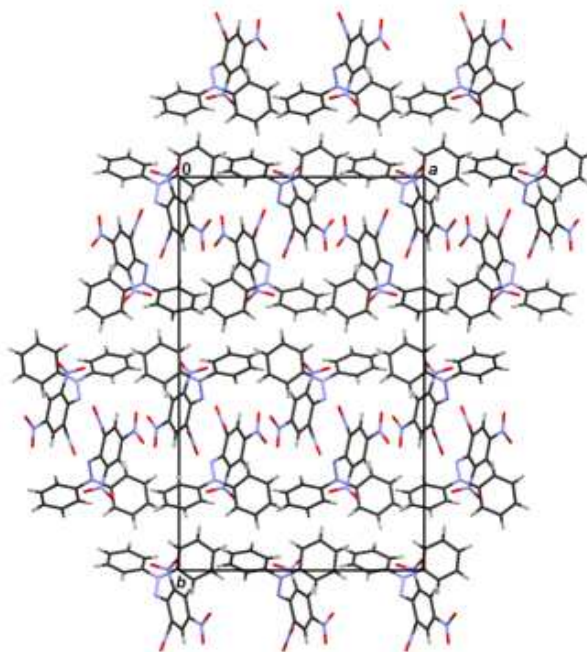


Figure 4: Crystal packing of DPPH1 viewed in the direction [001]. C–H...O hydrogen bonds have been omitted for clarity.

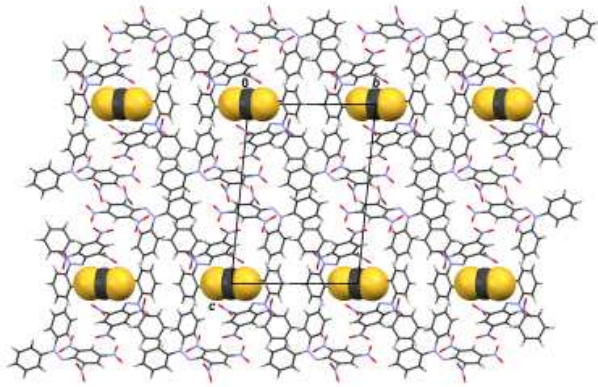


Figure 5: Crystal packing of DPPH2 showing channels containing molecules of CS_2 that run in the direction $[100]$. For clarity, CS_2 molecules are shown as van der Waals spheres.

216 The temperature dependence of the linewidth was ex-
 217 amined in the range $T = 10\text{--}297$ K. The results showed
 218 no significant changes of this parameter. The singlet
 219 line at $T = 10$ K had approximately the same width
 220 $W = (0.14 \pm 0.01)$ mT as the line at $T = 297$ K. How-
 221 ever, in contrary to the isotropic spectral line at room
 222 temperature, the measurements at 10 K showed the
 223 anisotropy of the spectrum. The angular variations of
 224 the g -value of the single crystal rotated along the three
 225 chosen orthogonal axes: a , b^* and c^* are shown in Fig-
 226 ure 6.

227 The elements of the $(\mathbf{g}^T \mathbf{g})_{ij}$ matrix at $T = 10$ K were
 228 determined from the experimental single-crystal data,
 229 by solving the following equation [21]:

$$g^2 = (\mathbf{g}^T \mathbf{g})_{aa} \sin^2 \theta \cos^2 \phi + (\mathbf{g}^T \mathbf{g})_{ab} \sin^2 \theta \sin 2\phi +$$

$$+ (\mathbf{g}^T \mathbf{g})_{bb} \sin^2 \theta \sin^2 \phi + (\mathbf{g}^T \mathbf{g})_{ac} \sin 2\theta \cos \phi +$$

$$+ (\mathbf{g}^T \mathbf{g})_{bc} \sin 2\theta \sin \phi + (\mathbf{g}^T \mathbf{g})_{cc} \cos^2 \theta \quad (1)$$

230 where θ and ϕ are the polar and azimuthal angles of
 231 the magnetic field vector \mathbf{B} in the $a - b^* - c^*$ coordi-
 232 nate system, respectively. The calculated g -tensor is
 233 presented in Figure 6 by solid lines. The principal val-
 234 ues of the g -tensor of DPPH1, obtained by diagonal-
 235 ization of the $\mathbf{g}^T \mathbf{g}$ matrix at $T = 10$ K, are shown in
 236 Table 5, with the estimated error ± 0.0001 . The ob-
 237 tained g -tensor is approximately axial with the max-
 238 imum value, $g_{xx} = 2.0046$, observed in the direction
 239 roughly parallel to the crystallographic a axis.

240 3.3.2. DPPH2

241 The single-crystals of DPPH2 showed the anisotropy
 242 singlet line already at room temperature. In compar-
 243 ison to DPPH1, the linewidth of DPPH2 was almost

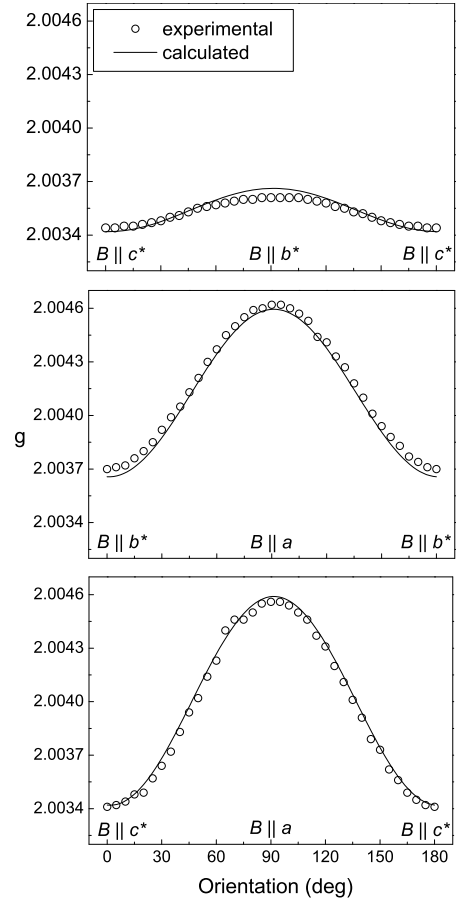


Figure 6: Angular variation of the g -values of EPR lines of the single crystal of DPPH1 at $T = 10$ K in three mutually perpendicular planes. Experimental values are given by circles and solid lines represent calculated g -values.

Table 5: Principal values of the g -tensors of DPPH1 and DPPH2.

	T (K)	g_{xx}	g_{yy}	g_{zz}
DPPH1	297	2.0036	2.0036	2.0036
	10	2.0046	2.0037	2.0034
DPPH2	297	2.0041	2.0036	2.0030
	10	2.0055	2.0040	2.0024
DPPH [22]	297	2.0037	2.0036	2.0034

244 halved: $W = (0.08 \pm 0.02)$ mT. This is in agreement
 245 with the fact that the solid state EPR spectrum of DPPH
 246 has a solvent dependent linewidth and that the lowest
 247 observed value of the linewidth was obtained for DPPH
 248 crystallized from CS_2 (0.15 mT for powder) [2]. Such
 249 a small value of the linewidth had earlier led to the con-
 250 clusion that the DPPH single crystals obtained from CS_2
 251 were probably solvent free, although there was no un-
 252 ambiguous evidence for that. The crystal structure data
 253 presented in this study have undoubtedly showed that
 254 DPPH2 has syncrystallized molecules of CS_2 : the unit
 255 cell contains four DPPH radicals and one CS_2 molecule.
 256 The obtained linewidth, in spite of the presence of the
 257 solvation, is very narrow (~ 0.18 mT for powder). The
 258 angular variations of the g -value of DPPH2 along the
 259 three orthogonal axes at $T = 297$ K are shown in Fig-
 260 ure 7. The dependencies obtained are in approximate
 261 agreement with the earlier measurements that had been
 262 performed round one axis for which crystallographic in-
 263 dices had not been given [23, 24].

264 Using the same method as for DPPH1, the $\mathbf{g}^T \mathbf{g}$ matrix
 265 was obtained and the principal values of the g -tensor
 266 of DPPH2 at $T = 297$ K were extracted and pre-
 267 sented in Table 5. The minimum value of the g -tensor,
 268 $g_{zz} = 2.0030$, was observed in the direction roughly par-
 269 allel to the crystallographic a axis.

270 The only up to now available experimental data for
 271 the g -tensor of DPPH crystallized from CS_2 , were ob-
 272 tained by Chirkov and Matevosyan [22]. They found
 273 different principal values of the g -tensors for the crys-
 274 tals prepared under different crystallization conditions
 275 (solvent purity, temperature, ...) and explained this
 276 effect by the crystal lattice defects. Otherwise, based
 277 on the fact that on raising the temperature right up to
 278 the melting point the EPR linewidth altered smoothly,
 279 the authors concluded that the crystals of DPPH had no
 280 solvent (CS_2) molecules included. One set of the prin-
 281 cipal values of the g -tensor obtained in the mentioned
 282 work is presented in Table 5, together with the corre-
 283 sponding values for DPPH1 and DPPH2. It could be
 284 seen that the g -tensor anisotropy obtained by Chirkov
 285 and Matevosyan [22] is significantly lower than the
 286 anisotropy obtained in this study. A reasonable explana-
 287 tion of the observed difference could be that the crystals
 288 grown from different experimental conditions had dif-
 289 ferent CS_2 : DPPH ratios and possibly, different crystal
 290 structures.

291
 292 The linewidth of $W = (0.15 \pm 0.04)$ mT obtained for
 293 DPPH2 at $T = 10$ K shows a significant broadening
 294 compared to the linewidth measured at room tempera-
 295 ture. That is in agreement with the earlier measurements

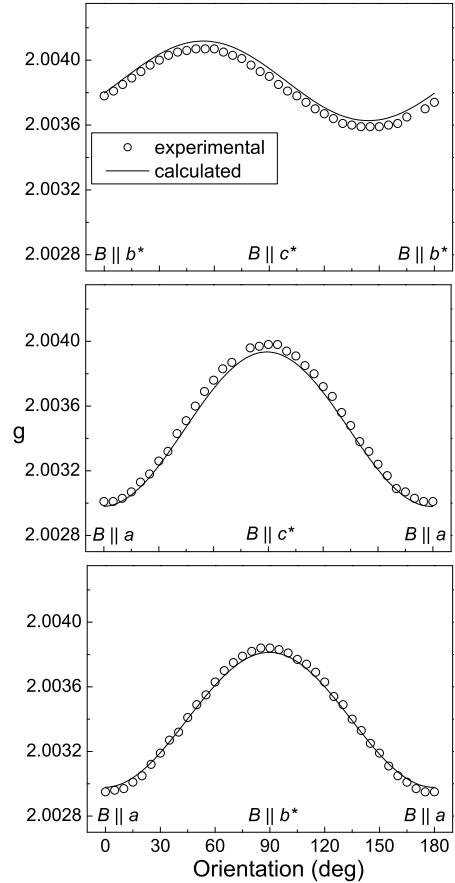


Figure 7: Angular variation of the g -values of EPR lines of the single crystal of DPPH2 at $T = 297$ K in three mutually perpendicular planes. Experimental values are given by circles and solid lines represent calculated g -values.

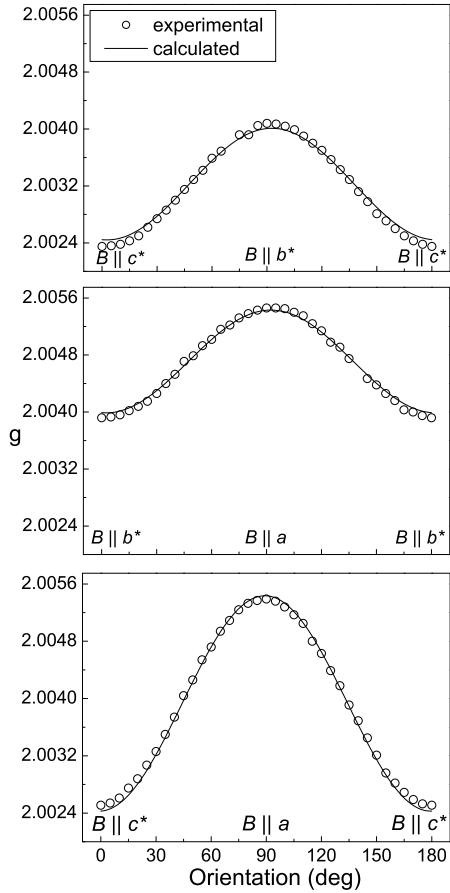


Figure 8: Angular variation of the g -values of EPR lines of the single crystal of DPPH2 at $T = 10$ K in three mutually perpendicular planes. Experimental values are given by circles and solid lines represent calculated g -values.

for the powder DPPH form [24, 25]. The angular variations of the g -value are shown in Figure 8.

The calculated principal values of the g -tensor of DPPH2 at $T = 10$ K are given in Table 5. The obtained g -tensor has the maximum value, $g_{xx} = 2.0055$, in the direction roughly parallel to the a axis. Comparing Figures 7 and 8, beside a change in magnitude of the principal values of the g -tensor, also a shift of the direction of eigenvectors could be observed. This effect had been indicated earlier [24].

3.4. Magnetization study

The temperature dependence of the molar magnetic susceptibility χ for DPPH1 and DPPH2 is presented in Figure 9. The two DPPH samples show almost identical behavior at temperatures above ≈ 150 K, but their behavior is qualitatively different at lower

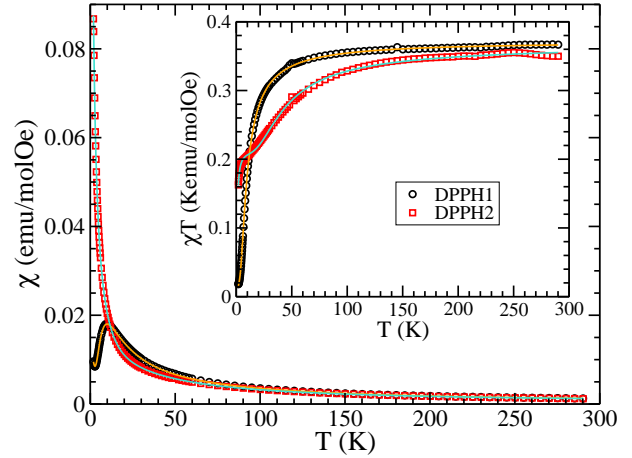


Figure 9: Temperature dependence of molar magnetic susceptibility for DPPH1 (black circles) and DPPH2 (red squares) compounds. Solid lines are the fitted curves. Inset: $\chi \cdot T$ vs T plot.

temperatures. For DPPH2, the molar susceptibility χ is decreasing monotonously with increasing temperature. For DPPH1, the susceptibility dependence on temperature curve attains a relatively broad maximum at $T_{max} = 10$ K. The decrease of the χ value with decreasing T below T_{max} points to the antiferromagnetic interactions in this compound.

In the inset of Figure 9 the temperature independent $\chi \cdot T$ value above 150 K was obtained after the diamagnetic corrections of -0.000180 and -0.000190 emu/mol for DPPH1 and DPPH2, respectively, were included. These values are in agreement with those in the previously published work [26]. From the $\chi \cdot T$ plots above 150 K the Curie constant values of 0.363 and 0.351 emuK/mol for DPPH1 and DPPH2, respectively, resulted. The values are close to the free electron value of 0.375 emuK/mol, and according to the EPR measurements, this should be the case also for DPPH1 and DPPH2. From the EPR data, using $g = 2.0036$, one can see that there are 96.5% radical electrons of the spin $S = 1/2$ per formula unit of DPPH1 and 93.3% radical electrons per formula unit of DPPH2. Approximately the same values for the Curie constant C result from the Curie-Weiss analysis of $\chi^{-1}(T) = (T - \theta)/C$, where the slope of the straight line gives $C = 0.373$ emuK/mol for DPPH1 and $C = 0.372$ emuK/mol for DPPH2. From here, the Curie-Weiss parameter θ amounts -5.3 and -13.8 K for DPPH1 and DPPH2, respectively. The negative values of this parameter point to the antiferromagnetic interactions in both samples. The obtained values are somewhat smaller than for other measured DPPH crystals, where the θ values were found to be from -22

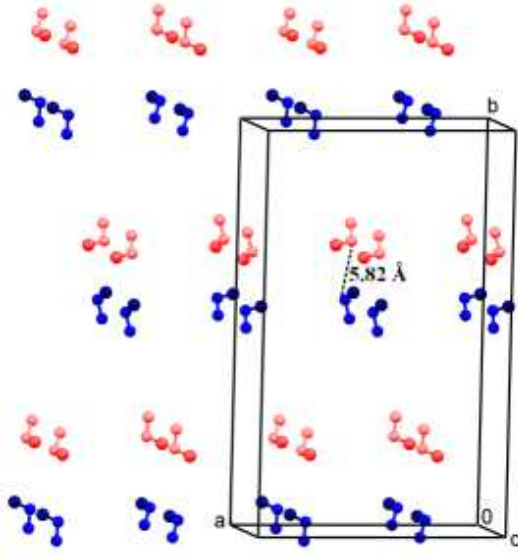


Figure 10: The closest distance between central N-atoms in the C-N-N fragments in the crystal structure of DPPH1. The closest distance is between two symmetry-independent molecules in the asymmetric unit. Molecules are color-coded: those labelled as **a** are red, lighter and **b** are blue, darker; carbon atoms are drawn in a darker shade.

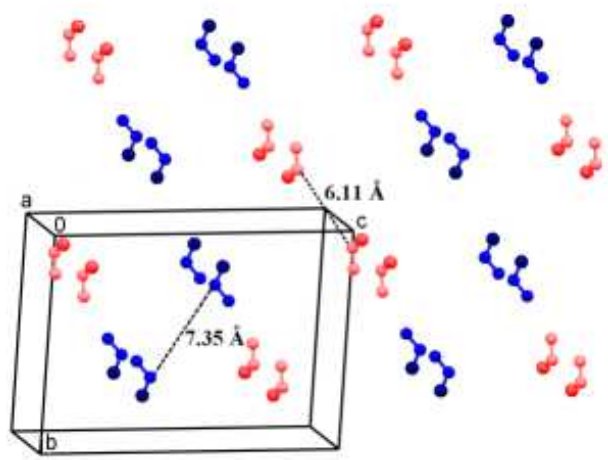


Figure 11: The closest distances between central N-atoms in the C-N-N fragments in the crystal structure of DPPH2. The closest distances are between pairs of molecules related by inversion centers. Molecules are color-coded: those labelled as **a** are red, lighter and **b** are blue, darker; carbon atoms are drawn in a darker shade.

to -26 K [27, 28]. However, it should be noted that these parameters are empirical and descriptive only, and might not give the true values of interaction energies.

The antiferromagnetic interactions for both compounds are indicated by the downward bending of the $\chi \cdot T$ curves with decreasing temperature (Figure 9). Magnetic correlations have visible effects starting approximately from 50 and 150 K for DPPH1 and DPPH2, respectively. Moreover, it seems that for DPPH2 there are two characteristic temperatures (energies). For further discussion of magnetic behavior of these compounds, their structural characteristics should be taken into account. It appears that consideration of the 3D long-range interactions would not be appropriate, as no pathways for such interactions could be observed in the crystal structures. Instead, a more precise interpretation of the magnetic data should be found in dimer interactions of radical electrons. Dimer approach was reported earlier for other DPPH crystals [26, 29]. Based on the crystal structures, such an approach is also justified for the present DPPH samples. Figures 10 and 11 present simplified schemes of magnetic interactions in DPPH1 and DPPH2 crystals, respectively. Only the C-N-N fragments are shown, with the closest distances between the central N atoms (according to the crystallographic and DFT studies, the unpaired electron is delocalized over the C1-N19-N20 bonds).

It is easy to notice that all molecules in DPPH1 are coupled into dimers (Figure 10). Pairs of symmetry independent molecules (in the same asymmetric unit) group into dimers with the centroid distances of 5.82 Å. Other paramagnetic neighbors are mutually much more distant (more than 7 Å).

In DPPH2 two kinds of dimers are observed (Figure 11). In this structure, the closest interactions are found between the pairs of molecules related by the inversion centers. Those labelled as **a** (red, lighter molecules) are mutually closer (6.11 Å) than those labelled as **b** (blue, darker molecules, 7.35 Å). It could be concluded that the DPPH2 molecules are divided into two types of dimers with different distances between the unpaired electrons, which could lead to different exchange parameters.

According to the previously mentioned, the susceptibility of DPPH1 is fitted by the following equation:

$$\chi(T) = w_1/2 \cdot \chi_{dim}(J) + w_2 \cdot \chi_{CW}, \quad (2)$$

where w_1 is the relative amount of molecules coupled into dimers and w_2 is the relative amount of single molecules interacting weakly with other neighboring molecules. The uncoupled single paramagnetic centers could originate from the defects and surface effects in the crystals. The susceptibility of dimers is given by:

$$\chi_{dim}(J) = 2N\mu_B^2 g^2 / kT (3 + \exp(-J/kT)), \quad (3)$$

where J is the Heisenberg exchange coupling (defined by the interaction Hamiltonian $\mathcal{H}_{INT} = -JS_1S_2$) between two unpaired electrons in a dimer [30]. Other

398 parameters have their usual meanings. The Curie-Weiss 446
399 molar susceptibility of weakly interacting spin $S = 1/2$ 447
400 molecules is: 448

$$\chi_{CW} = N\mu_B^2 g^2 / 4k(T - \theta). \quad (4)$$

401 When $g = 2.0036$ is assumed in accordance with 449
402 the EPR determination, the best fit is achieved with
403 $w_1 = 0.870$ and $w_2 = 0.0944$. At the same time, the ob- 450
404 tained antiferromagnetic exchange coupling within the 451
405 dimers is $J = -17.5$ K and the long-range interaction 452
406 Curie-Weiss parameter $\theta = -1.89$ K. The agreement 453
407 between the measured data and the fitted function is ex- 454
408 cellent in the whole interval of temperature (see Figure 455
409 9). The value of J is close to the already published data 456
410 on other DPPH crystals [26, 29]. 457

411 The DPPH2 susceptibility was analyzed assuming the 458
412 coexistence of two kinds of dimers with different ex- 459
413 change couplings. Therefore, the data were fitted by: 460

$$\chi(T) = w_1/2 \cdot \chi_{dim}(J_1) + w_2/2 \cdot \chi_{dim}(J_2), \quad (5)$$

414 where w_1 and w_2 are the relative amounts of molecules 463
415 coupled into particular types of magnetic dimers with 464
416 the exchange energies J_1 and J_2 , respectively. The ob- 465
417 tained parameters are $w_1 = 0.570$ and $w_2 = 0.402$, 466
418 whereas the corresponding exchange interactions are 467
419 $J_1 = -1.56$ K and $J_2 = -83.9$ K. In Figure 11, J_1 and 468
420 J_2 could be associated with the molecules labelled as **b** 469
421 (blue, darker molecules) and **a** (red, lighter molecules), 470
422 respectively. 471

423 The fitting of the $\chi \cdot T$ curves (inset in Figure 9) 472
424 gave consistently the same parameters for both com- 473
425 pounds. However, the obtained results for the exchange 474
426 parameters for DPPH1 ($J = -17.5$ K) and for the **a** 475
427 labelled molecules in DPPH2 (red, lighter molecules, 476
428 $J_2 = -83.9$ K), which have approximately the same mu- 477
429 tual distance within dimers, are significantly different. 478
430 The difference arises from the different orientation of 479
431 molecules in DPPH1 and DPPH2. The molecules form- 480
432 ing dimers in DPPH1 are almost mutually perpendicular 481
433 (the angle between the planes which are determined by 482
434 the C-N-N fragment, is 80.4°) and the molecules form- 483
435 ing dimers in DPPH2 are mutually parallel (for both 484
436 types of dimers). 485

437 It is worth mentioning that the molecular field model 486
438 in which the neighboring dimers mutually interact gave 487
439 poor agreement with the measured data. The possi- 488
440 ble explanation lies in the fact that at low temperatures 489
441 the antiferromagnetically coupled dimers are in the sin- 490
442 glet state, and their mutual interactions are therefore un- 491
443 likely. 492

444 The magnetic susceptibility analysis showed the pres-
445 ence of magnetic dimerization in both DPPH1 and

DPPH2, but the amounts of entities participating and
the strength of exchange couplings are different for the
two samples, in accord with their crystal structures.

4. Conclusions

Crystal structures for two DPPH samples were
solved: DPPH1, crystallized from ether, and DPPH2,
crystallized from CS_2 . The single-crystal X-ray diffrac-
tion analysis (and also IR spectroscopy) showed that the
single crystals of DPPH1 are solvent free and those of
DPPH2 contain one molecule of CS_2 in the unit cell.
From the EPR measurement principal values of the g -
tensors at room (297 K) and low (10 K) temperatures
were obtained. Although the crystals of DPPH2 give a
narrower linewidth, the crystals of DPPH1, due to an
almost insignificant change of linewidth with decreas-
ing temperature (from room temperature to $T = 10$ K)
and a lower g -tensor anisotropy, prove to be more suit-
able as the EPR probe. The magnetization study show
pairing into dimers with the antiferromagnetic exchange
coupling of -17.4 K for all molecules in DPPH1 and
pairing into two kinds of dimers (*ca* 50-50%) with the
antiferromagnetic exchange couplings of -1.56 K and
 -83.9 K, in DPPH2. The magnetization results are
in accordance with the crystal structures of the com-
pounds.

The results presented in this study contribute to better
understanding of the properties of DPPH, which is im-
portant regarding the great significance of DPPH in the
EPR spectroscopy.

Acknowledgments

D. Žilić is grateful to D. Merunka for the useful dis-
cussion. This research was supported by the Min-
istry of Science, Education and Sports of the Republic
of Croatia (projects 098-0982915-2939, 098-0982904-
2946, 098-1191344-2943 and 119-1191458-1017).

References

- [1] J. Krzystek, A. Sienkiewicz, L. Pardi, L. C. Brunel, J. Magn. Reson. 125 (1997) 207–211.
- [2] N. D. Yordanov, Appl. Magn. Reson. 10 (1996) 339–350.
- [3] J. X. Boucherle, B. Gillon, J. Maruani, J. Schweizer, Acta Crystallogr. C 43 (1987) 1769–1773.
- [4] J. A. Weil, J. K. Anderson, J. Chem. Soc. (1965) 5567–5570.
- [5] F. H. Allen, Acta Crystallogr. B 58 (2002) 380–388.
- [6] C. T. Kiers, J. L. de Boer, R. Olthof, A. L. Spek, Acta Crystallogr. B 32 (1976) 2297–2305.
- [7] D. E. Williams, J. Am. Chem. Soc. 89 (1967) 4280–4287.
- [8] D. E. Williams, J. Chem. Soc. (1965) 7535–7536.

- 493 [9] B. Rakvin, M. Požek, A. Dulčić, *Solid State Commun.* 72 (2)
494 (1989) 199–201.
- 495 [10] B. Rakvin, T. A. Mahl, A. S. Bhalla, Z. Z. Sheng, N. S. Dalal,
496 *Phys. Rev. B* 41 (1) (1990) 769–771.
- 497 [11] B. Rakvin, D. Žilić, N. S. Dalal, J. M. North, P. Cevc, D. Arčon,
498 K. Zadro, *Spectrochim. Acta A* 60 (2004) 1241–1245.
- 499 [12] CrysAlis PRO, Oxford Diffraction Ltd., U. K., 2007.
- 500 [13] G. M. Sheldrick, *Acta Crystallogr. A* 64 (1) (2008) 112–122.
- 501 [14] A. L. Spek, PLATON98: A Multipurpose Crystallographic Tool,
502 University of Utrecht, The Netherlands, 1998.
- 503 [15] L. J. Farrugia, *J. Appl. Cryst.* 30 (1997) 565.
- 504 [16] C. F. Macrae, P. R. Edgington, P. McCabe, E. Pidcock, G. P.
505 Shields, R. Taylor, M. Towler, J. van de Streek, *J. Appl. Cryst.*
506 39 (2006) 453–457.
- 507 [17] S. M. Mattar, J. Sanford, *Chem. Phys. Lett.* 425 (2006) 148–153.
- 508 [18] N. S. Dalal, D. E. Kennedy, C. A. McDowell, *Chem. Phys. Lett.*
509 30 (1975) 186–189.
- 510 [19] R. M. Silverstein, C. G. Bassler, T. C. Morrill, *Spectrometric*
511 *Identification of Organic Compounds*, 3rd Edition, John Wiley
512 and Sons, Inc., New York, 1974.
- 513 [20] K. Nakamoto, *Infrared and Raman Spectra of Inorganic and Co-*
514 *ordination Compounds*, 5th Edition, John Wiley and Sons, Inc.,
515 New York, 1997.
- 516 [21] J. A. Weil, J. R. Bolton, J. E. Wertz, *Electron Paramagnetic Res-*
517 *onance*, John Wiley and Sons, Inc., New York, 1994.
- 518 [22] A. K. Chirkov, R. O. Matevosyan, *J. Struct. Chem.* 11 (2) (1970)
519 242–246.
- 520 [23] C. Kikuchi, V. W. Cohen, *Phys. Rev.* 93 (3) (1954) 394–399.
- 521 [24] L. S. Singer, C. Kikuchi, *J. Chem. Phys.* 23 (1955) 1738–1739.
- 522 [25] P. Swarup, B. N. Misra, *Z. Phys.* 159 (1960) 384–387.
- 523 [26] J. W. Duffy, D. L. Strandburg, *J. Chem. Phys.* 46 (2) (1967)
524 456–464.
- 525 [27] A. V. Itterbeek, M. Labro, *Physica* 30 (1) (1964) 157–160.
- 526 [28] J. W. Duffy, *J. Chem. Phys.* 36 (2) (1962) 490–493.
- 527 [29] J. W. Duffy, D. L. Strandburg, J. F. Deck, *J. Chem. Phys.* 68 (5)
528 (1978) 2097–2104.
- 529 [30] O. Kahn, *Molecular Magnetism*, Wiley-VCH Inc., New York,
530 1993.